Nucleon-Nucleon Total Cross Sections from 1.1 to 8 GeV/c

D. V. Bugg, D. C. Salter, and G. H. Stafford
Rutherford High Energy Laboratory, Chilton, Berkshire, England

AND

R. F. George, K. F. Riley, and R. J. Tapper
Cavendish Laboratory, Cambridge, England

(Received 26 January 1966)

Measurements have been made of the total cross sections $\sigma(p$-$p)$ and $\sigma(p$-$d)$ over the laboratory momentum range 1.1 to 8 GeV/c, with relative errors of 0.1%. The absolute accuracies of these cross sections are limited to 0.3% by lack of information which will allow the Coulomb-nuclear interference to be calculated accurately. Values of the total cross sections $\sigma(p$-$n)$ and $\sigma(I=0)$ are deduced by assuming the Glauber correction. Structure is observed in $\sigma(p$-$p)$ near a mass value of 2.75 GeV/c^2; its interpretation is discussed. $\sigma(I=0)$ rises rapidly in the range 2.3 to 2.9 GeV/c^2, and this is attributed to the onset of strong inelastic scattering.

1. INTRODUCTION

THE aim of this experiment was to measure p-p and p-d total cross sections, referred to here as $\sigma(p$-$p)$ and $\sigma(p$-$d)$, with an absolute accuracy of about 0.1%, and over as large a momentum range as was available at Nimrod. The conventional transmission technique was used. In previous experiments,[1-6] $\sigma(p$-$p)$ has been measured with an accuracy of a few percent, but information on $\sigma(p$-$n)$ has been rather scanty. There have been some measurements of $\sigma(p$-$d)$,[1,4,5,7] and a few direct ones of $\sigma(n$-$p)$ using neutron beams.[8,9] The situation has been confused by large systematic differences between results obtained by different groups. Also, because most groups have covered only a small range of momentum, it has been difficult to get an integrated picture of the variation of $\sigma(p$-$n)$ with energy.

2. EXPERIMENTAL

The traditional transmission technique for measuring total cross-sections is well known.[10] The transmission is measured with a number of closely spaced counters subtending a range of solid angles at the target, and the total cross section is obtained by extrapolating the partial cross sections so determined to zero solid angle. The experimental layout used in this experiment is shown diagrammatically in Fig. 1.

The sizes of the transmission counters are determined by the requirements that (a) they should encompass all of the unscattered beam, (b) losses due to single and multiple Coulomb scattering should be small, and (c) they should fall well within the angular range of nuclear elastic and inelastic scattering, so that the extrapolation to zero solid angle is approximately linear. To a first approximation, nuclear and Coulomb scattering are both functions of the transverse momentum, $p_T \simeq p\theta$, only, and are independent of energy; here p is the beam momentum and θ the scattering angle. Coulomb and nuclear scattering are approximately equal when $p_T = 40$ MeV/c; the cross section for single Coulomb scattering through values of p_T larger than this is approximately 0.2 mb. The angular distribution for p-p elastic scattering varies[11,12] approximately as $\exp(10t)$, where $t \simeq -p_T^2$ in $(\text{GeV}/c)^2$; the angular distribution of products from inelastic scattering is similar. Hence both fall by about 10% between $p_T = 0$ and 100 MeV/c. It is

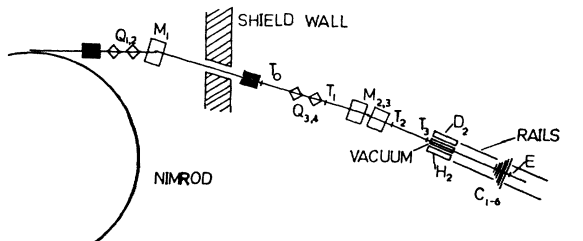

FIG. 1. The experimental layout. M and Q denote bending and quadrupole magnets. T_{1-3} are scintillation counters used to define the beam. C_{1-6} are the transmission counters and E the efficiency counter.

[1] F. F. Chen, C. P. Leavitt, and A. N. Shapiro, Phys. Rev. **103**, 211 (1956).
[2] M. J. Longo and B. J. Moyer, Phys. Rev. **125**, 701 (1962).
[3] V. P. Dzhelepov, V. I. Moskalev, and S. V. Medved', Dokl. Akad. Nauk. **104**, 380 (1955).
[4] A. N. Diddens, E. Lillethun, G. Manning, A. E. Taylor, T. G. Walker, and A. M. Wetherell, Phys. Rev. Letters **9**, 32 (1962).
[5] W. Galbraith, E. W. Jenkins, T. F. Kycia, B. A. Leontić, R. H. Phillips, A. L. Read, and R. Rubinstein, Phys. Rev. **138**, B913 (1965).
[6] S. J. Lindenbaum, W. A. Love, J. A. Niederer, S. Ozaki, J. J. Russell, and L. C. L. Yuan, Phys. Rev. Letters **7**, 185 (1961).
[7] V. P. Dzhelepov, V. I. Satarov, and S. M. Golovin, Dokl. Akad. Nauk. **104**, 717 (1955).
[8] V. S. Pantuev, M. N. Khachaturyan, and I. V. Chuvilo, Yadern. Fiz. **1**, 134 (1965) [English transl.: Soviet J. Nucl. Phys. **1**, 93 (1965)].
[9] H. Palevsky, J. L. Friedes, R. J. Sutter, R. E. Chrien, and R. H. Muether, *Proceedings of the Congrès International de Physique Nucléaire, 1964*, edited by Mme P. Gugenberger (Editions du Centre National de la Recherche Scientifique, Paris, 1964), Vol. II, p. 162.
[10] See, for example, U. Amaldi, T. Fazzini, G. Fidecaro, C. Ghesquière, M. Legros, and H. Steiner, Nuovo Cimento **34**, 825 (1964).
[11] K. J. Foley, S. J. Lindenbaum, W. A. Love, S. Ozaki, J. J. Russell, and L. C. L. Yuan, Phys. Rev. Letters **11**, 425 (1963).
[12] A. N. Diddens, E. Lillethun, G. Manning, A. E. Taylor, T. G. Walker, and A. M. Wetherell, Phys. Rev. Letters **9**, 108 (1962).

convenient, therefore, to cover the range $p_T = 50$ to 150 MeV/c with the transmission counters. To achieve this in the present experiment, they were mounted on a trolley running parallel to the beam line, and their distance from the target was made proportional to the momentum, so that they always intercepted particles over the same range of p_T.

The total cross section is obtained from the ratio, (t_e/t_f) of the transmission through empty and full targets according to the relation

$$\sigma = (1/Nl) \ln(t_e/t_f). \quad (1)$$

Here l is the length of the target and N the number of atoms per unit volume in it. In this experiment three identical target vessels were used; the first contained liquid hydrogen, the second liquid deuterium, and the third was evacuated. In a separate calibration run, the transmission was measured through the three targets empty, and was found to be the same for all three within 0.01%.

Most corrections are eliminated by taking the ratio (t_e/t_f) and extrapolating to zero solid angle. The latter eliminates double scattering in the target, for example. The former eliminates most instrumental defects, which should be the same for target full and empty. For example, the proton beam is attenuated appreciably by p-n charge exchange in the transmission counters. However, this effect cancels out in the ratio (t_e/t_f), provided that the energy loss in the full target causes only a negligible change in the charge-exchange cross section.

Care is necessary in the design of the apparatus to ensure that any instrumental effect, involving the efficiency with which scattered particles are detected, extrapolates to zero at zero solid angle. In this context, we mention particularly conversion of neutrons in successive transmission counters; for example, those produced in the reaction $pp \to pn\pi^+$ are peaked along the beam direction, and many of them hit the transmission counters. In a first approximation, the number of neutrons counted is proportional to the weight of material they have traversed. It is thus necessary to arrange that the area of overlap of counters and light guides on succeeding counters follows a progression which extrapolates to zero at counter zero. Essentially, this means making the area of the ith counter proportional to i. This was done in the present experiment, but appears to have been overlooked in most previous ones.

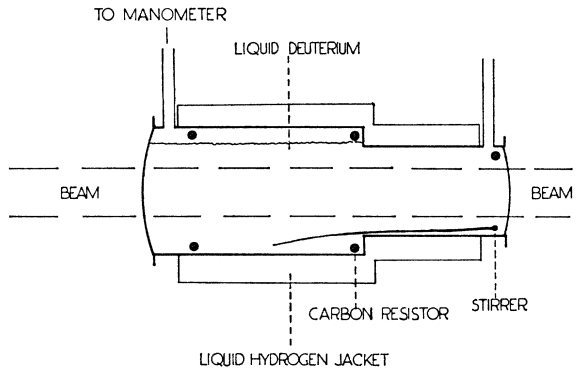

FIG. 2. The liquid-deuterium target.

(a) The Beam

The beam was that originally set up by Taylor *et al.*[13] for the study of Coulomb-nuclear interference in pp elastic scattering. The internal proton beam of Nimrod was scattered from a beryllium target located in one of the magnet octants. Beams of different momenta were obtained by varying the Nimrod internal energy. The first collimator accepted protons scattered elastically at 67 mrad to the primary beam. Momentum separation was provided by the bending magnet $M1$, which deflected the beam through 50 mrad on to the second collimator, a channel 2.5 cm high, 9 mm wide, and 150 cm long. The quadrupole doublet $Q1$ and $Q2$ focused the beam on to this collimator, and $Q3$ and $Q4$ refocused it on to the small counter E behind the transmission counter array. The momentum of the beam was determined by the two bending magnets $M2$ and $M3$, and the telescope of scintillation counters $T1$, $T2$, and $T3$. The magnets were calibrated by floating-wire measurements and with a rotating-coil magnetometer to an absolute accuracy of $\pm 0.5\%$ and with relative errors between momenta of $\pm 0.2\%$. The magnet currents were stable to better than $\pm 0.2\%$.

Theoretically no pions should be able to get down the beam line. A pion contamination of less than 1 per 10^4 protons was established by time-of-flight measurements below 2.5 GeV/c, and at higher momenta using a Čerenkov counter.[14] Beam intensities were typically 4×10^4/pulse at the highest momenta, falling to 1000/pulse at the lowest.

(b) The Target

The target vessel is shown in Fig. 2. The cylindrical body was made of stainless steel and was 55 cm long. A jacket of liquid hydrogen was used to refrigerate the target liquid, which was completely closed off and quiescent. The target and jacket were suspended from a hydrogen reservoir which was surrounded by a tank of liquid nitrogen. Heat loss to the target was reduced by two copper shields, the inner one attached to the hydrogen jacket, and the outer one to the nitrogen reservoir. The end windows were circular Melinex sheets, 4 in. in diam and 0.005 in. thick at the entrance end, and 7 in. in diam and 0.010 in. thick at the exit end. Across the apertures in both heat shields six separated sheets of 0.001.-in. thick Melinex, coated with aluminium, were attached to act as a radiation shield.

The location of the target in the vacuum vessel was

[13] A. E. Taylor, A. Ashmore, W. S. Chapman, D. F. Falla, W. H. Range, D. B. Scott, A. Astbury, F. Capocci, and T. G. Walker, Phys. Letters 14, 54 (1965).

[14] We are grateful to Dr. Hultschig and his team, visiting from DESY, for help in measuring the beam contamination.

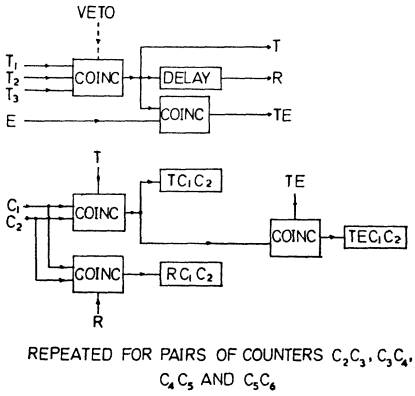

FIG. 3. A block diagram of the electronics.

checked by surveying the positions of crosses painted on the target windows, and viewed through slits in the radiation shields. The length was measured by viewing the end windows with a traveling telescope through small ports in the side of the vacuum tank. The curvature of the windows was found from measurements with a dial gauge, with the target pressurized with air to produce the same bowing as when it was filled with liquid hydrogen.

The vapor pressure above the liquid surface was measured using a mercury manometer. The corresponding density was deduced from tables compiled by Tapper.[15] A catalyst consisting of pellets of 6% nickel on alumina was put into the target to speed conversion to the equilibrium state (largely para for hydrogen and ortho for deuterium). Measurements were made on gas samples drawn from the target of the ortho-para ratio, using an apparatus similar to that of Grilly.[16] Five carbon resistors placed around the periphery of the target were used to measure the temperature distribution in the liquid. A paddle was provided for mechanically stirring the target liquid. However, temperature differences between the resistors were found to be <0.01°C, and the paddle was not used.

The vacuum target was identical to the others apart from the absence of liquid reservoirs. The jacket surrounding this target was also evacuated.

The three targets were mounted on a framework which could be moved perpendicular to the beam line to bring each target into the beam in turn.

At each momentum, measurements were also made of the attenuation of the beam by a cylinder of aluminum of radius 2 in. and length 4 cm, which was placed in front of the vacuum target. Any genuine small structure in $\sigma(p\text{-}p)$ or $\sigma(p\text{-}n)$ should be smeared out by the Fermi motion in the aluminum nucleus, and would not be seen. This was intended largely as a check on the apparatus.

[15] R. J. Tapper, Rutherford Laboratory Report NIRL/R/95 (unpublished).

[16] E. R. Grilly, Rev. Sci. Instr. **24**, 72 (1953).

TABLE I. The dimensions of the scintillators.

Counter	Height×width×thickness (cm)
T_0	5.0×2.5×1.25
T_1	7.0×2.5×0.2
T_2	7.0×4.0×0.2
T_3	5.0×3.2×0.2
C_1	20 diam×1.25
C_2	$20\sqrt{2}$ diam×1.25
C_3	$20\sqrt{3}$ diam×1.25
C_4	$20\sqrt{4}$ diam×1.25
C_5	$20\sqrt{5}$ diam×1.25
C_6	55.9×46.0×1.25
E	5.0×2.5×0.3

(c) The Counters and Electronics

The electronic logic is outlined schematically in Fig. 3; standard Rutherford Laboratory and Atomic Energy Research Establishment 2000 Series equipment was used. The dimensions of the scintillation counters are given in Table I. A coincidence, which we call T, between T_1, T_2, and T_3 was used to define the incident beam. The largest of the three beam-defining counters, T_2, counted nearly all of the particles in the beam line at all momenta. The dead time of the discriminator on T_2 was set to 120 nsec and defined the over-all dead time of the whole electronic system.

There were six transmission counters C_{1-6}. The first five were $\frac{1}{2}$-in. thick circles of scintillator of diameter $8\sqrt{i}$ in., where $i=1\cdots5$, embedded in rectangular Perspex light guides. The sixth counter C_6 was a rectangle of scintillator. To minimize the effect of Čerenkov light produced in the light guides, successive pairs of transmission counters were taken in threefold coincidence TC_iC_{i+1} with the beam pulse T. This also eliminated any troubles due to after-pulsing in the 56 AVP photomultipliers; some after-pulsing was observed in the largest three counters C_{4-6}. The widths of the TCC resolution curves were adjusted to be the same within 0.1 nsec; this ensured that they all counted the same spectrum of scattered particles.

The small counter E was used to monitor continuously the efficiencies of the transmission counters. By putting TE into coincidence with TCC, the efficiency of the complete system, scintillator+photomultipliers+electronics, was monitored. A valuable running check on the electronics was that the efficiency of one counter measured by TE in coincidence with TC_i was the same for both channels on which C_i was present.

The only significant source of accidental coincidences was due to two protons traversing the beam-line within the resolving time of the TCC coincidences. We refer to these as twofold accidentals. They were monitored by delaying the T pulse by about 200 nsec (we refer to this as the R pulse), and recording RC_iC_{i+1} coincidences. With beam intensities of 5×10^4 per 300-msec pulse, twofold accidentals could be as high as 1% of true coincidences. Because there is always some uncertainty in correcting for randoms, an arrangement similar to

that of Citron *et al.*[17] was used to eliminate them electronically at all but the lowest momenta, where they were negligible. Two systems (Fig. 4) were used in parallel to veto the T pulse whenever two beam particles were recorded in counter T_0 within 15 nsec of one another. The first of these was a fast gate. The first particle in T_0 opened the gate, and a veto resulted from a second anywhere within the time interval 3 to 15 nsec afterwards. This device had a negligible dead time. The second system used a fan-out to split the T_0 photomultiplier pulse four ways. These four ways were recombined in an analog adder with appropriate delays between them, so as to generate an approximately square output, 15 nsec long. The ripple on the square wave was $<10\%$. If a second particle traversed T_0 anywhere within these 15 nsec it produced a second pulse which added on to the top of the square wave, and triggered a discriminator set above the level of square waves due to single particles. This device, unlike the first, worked when two particles traversed T_0 within 3 nsec, but it was more difficult to establish its efficiency. Also, the discriminator had a dead time of about 40 nsec. The two devices together are believed to have vetoed twofold accidentals with an efficiency $>98\%$, and the loss of beam was less than 5%.

Two small counters T_p and T_p' were used for measuring beam profiles over the target entry window and over the transmission array.

3. COLLECTION AND TREATMENT OF DATA

Data were taken at 40 momenta in the range between 1.1 and 7.8 GeV/c. Consistency checks were made at several momenta over this range and results were reproducible with an absolute accuracy of about $\pm 0.1\%$. At each momentum, the data were collected in five or six batches which were checked for statistical consistency and then averaged. The momentum spread in the beam was typically $\pm 0.5\%$. The statistical accuracy on the cross sections was $\leqslant \pm 0.1\%$ at most momenta.

The efficiency of each pair of transmission counters C_iC_{i+1} was determined from the ratio TEC_iC_{i+1}/TE. Corrections were applied to the data for

(i) variations of efficiency over the areas of the transmission counters,
(ii) Čerenkov counts,
(iii) randoms, where necessary,
(iv) single and multiple Coulomb scattering,
(v) Coulomb-nuclear interference.

Cross sections were determined by extrapolating the data to zero solid angle, (vi), and were corrected for

(vii) changes in the density of the air between the target and the counters in the time between target full and empty runs, and
(viii) the ortho-para ratio and purity of the deuterium.

[17] A. Citron, W. Galbraith, T. F. Kycia, B. A. Leontić, R. H. Phillips, and A. Rousset, Phys. Rev. Letters **13**, 205 (1964).

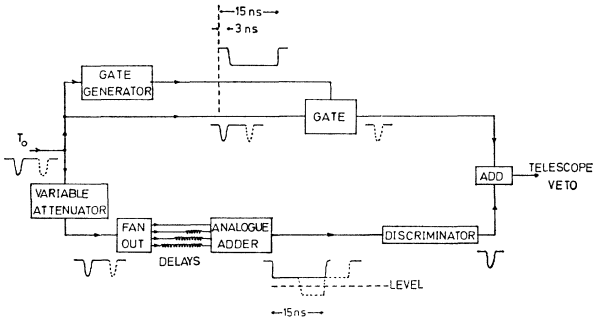

FIG. 4. The electronic system used to eliminate twofold accidentals.

Finally, $\sigma(p\text{-}n)$ and $\sigma(I=0)$ were deduced, taking into account

(ix) the Glauber correction, and
(x) Fermi motion of the nucleons in the deuteron.

(i) Variations of Efficiency over Scintillator Areas

Scattered particles reaching the transmission counters were recorded with different efficiencies from unscattered particles, because of the variation of efficiency over the areas of the counters. Correction was made for this in a straightforward fashion. It was a small correction since (a) few scattered particles hit the transmission counters, and (b) the efficiency was always over 99% for counting beam particles, and was higher still over the remaining area.

EHT and discriminator levels were left constant throughout the experiment, and it was observed that the efficiency ϵ for counting beam particles obeyed a relation

$$\ln(1-\epsilon)=A+B/\beta^2, \tag{2}$$

where A and B were constants for any one counter, and β was the velocity of beam particles. This is approximately what would be expected from a Poisson pulse-height distribution and an energy loss proportional to $1/\beta^2$ in the scintillator.

(ii) Čerenkov Counts

Scattered particles traversing the light guides of transmission counters produced Čerenkov light, which could be counted with low efficiency. This was minimized by overlapping successive light guides as little as possible, and taking triple coincidences TC_iC_{i+1}, as described in Sec. 2 above. Measurements were made at 7 GeV of the efficiency, ϵ_c, for counting Čerenkov light, where the guide of one counter overlapped the scintillator of the next, and a correction was applied by relating $\ln\epsilon_c$ along the lines of Eq. (2), to the known variation of the intensity of Čerenkov light with β. The quantity ϵ_c was immeasurably small for the first two counters, and rose to 1% at 7 GeV in the case of the largest counter.

(iii) Randoms

The only accidental coincidences of any significance were twofold accidentals. As mentioned in Sec. 2(c) above, they were eliminated electronically at most momenta.

Let α_i be the probability that a particle traverses the target and is recorded in the ith counter and let r_i be the number of randoms recorded by the delayed coincidence RC_iC_{i+1}. Then, if the efficiency of the veto system is e, the number of random coincidences, n_r, is

$$n_r=\tfrac{1}{2}(1-e)r_i(1-\alpha_i).$$

The factor of $\frac{1}{2}$ comes from the fact that the first of two particles in twofold accidental coincidence will produce the T pulse, and the second one can lie only within the second half of the coincidence resolution curve. At no momentum did this correction exceed 0.01% when the veto was used, or 0.1% when it was not used.

(iv) Single and Multiple Coulomb Scattering

Since the single Coulomb scattering cross-section varies as $1/\theta^4$ for small θ, the number of beam particles scattered so as to miss a counter subtending an angle θ at the target varies as $1/\theta^2$. This does not extrapolate to zero as $\theta\rightarrow 0$, and correction has to be made for it before the extrapolation is performed. Let the radius of counter i be R_i, and suppose the trajectory of a beam particle intersects the counter at a distance r_i from its axis. Then the Coulomb correction is

$$d\sigma(\text{Coulomb})=\frac{-4\pi(\alpha\hbar c)^2}{p^2\theta_i^2\beta^2}\left\{\left\langle\left(1-\frac{r_i^2}{R_i^2}\right)^{-2}\right\rangle+\frac{2d_i^2\langle\theta^2\rangle}{R_i^2}\times\left\langle\left(1+\frac{2r_i^2}{R_i^2}\right)\left(1-\frac{r_i^2}{R_i^2}\right)^{-4}\right\rangle\right\}. \quad (3)$$

Here α is the fine-structure constant, and p and β are the laboratory momenta and velocities of beam particles. Braces indicate averages over the beam profile at counter surfaces. The first term is an exact correction for finite beam size. The second one is a first-order correction for the fact that particles which are single-Coulomb-scattered are also subject to multiple Coulomb scattering. In Eq. (3), $\langle\theta^2\rangle$ is the mean-square angle of multiple scattering, and d_i is the distance from counter i to the center of the target. For hydrogen and deuterium, the Coulomb correction to the cross section was always less than 0.4% in the smallest counter, for which the factor in curly brackets was typically 1.05. For aluminum, however, the Coulomb correction was an order of magnitude larger, and the factor in curly brackets rose to 1.4 for the smallest counter. No correction was necessary for multiple Coulomb scattering alone, even for aluminum.

(v) Coulomb-Nuclear Interference

The cross section for Coulomb scattering equals that for nuclear elastic scattering when $p\theta\simeq 40$ MeV/c. In this experiment, the five transmission counters counted particles over a range of p_T roughly up to 70 MeV/c for $i=1$ and 150 MeV/c for $i=5$. Thus, although the correction for single Coulomb scattering was very small, and could be made with confidence, that for Coulomb-nuclear interference was much larger, and less certain. This interference term is

$$d\sigma(\text{CN})=\int_{\theta_i}^{\infty}\frac{8\pi\alpha\hbar c}{p\beta\theta^2}\left\{\text{Re}f(\theta)+\frac{2\alpha}{\beta}\ln\left(\frac{1.06}{ka\theta}\right)\text{Im}f(\theta)\right\}\theta d\theta, \quad (4)$$

where $f(\theta)$ is the spin-averaged nuclear scattering amplitude, k is the wave number of the incident beam, and a the radius characteristic of the nucleon for elastic scattering. Because of the factor α in it, the second term in the bracket in (4) is negligibly small over the range of θ involved in this experiment, and it will not be considered further. $\text{Im}f(\theta)$ is well known from the optical theorem, and experiments[11,12] on elastic scattering. However, very little is known about $\text{Re}f(\theta)$. There have been experiments[13,18–22] on Coulomb-nuclear interference in p-p scattering, and the results agree fairly well with a calculation by Söding[23] based on dispersion relations. We have therefore used his calculated values for $\text{Re}f_{pp}(0)$ over our entire momentum range. In the case of deuterium, there will be coherent interference between $\text{Re}f_{pn}(\theta)+\text{Re}f_{pp}(\theta)$ and the amplitude for Coulomb scattering from the deuteron. Unfortunately, there are no data at all on $\text{Re}f_{pn}(\theta)$ in this momentum region. Values of $\text{Re}f_{pn}(0)$ have been calculated from forward dispersion relations.[24] These values are used in correcting the deuterium results for Coulomb interference. In the absence of any information on the angular dependence of $\text{Re}f(\theta)$ we have assumed

$$\text{Re}f(\theta)=\text{Re}f(0)e^{4.6t} \quad (5)$$

in accord with the known angular dependence of $\text{Im}f_{pp}(\theta)$.

It is convenient to break up the Coulomb-nuclear

[18] E. Lohrmann, H. Meyer, and H. Winzeler, Phys. Letters **13**, 78 (1964).

[19] K. J. Foley, R. S. Gilmore, R. S. Jones, S. J. Lindenbaum, W. A. Love, S. Ozaki, E. H. Willen, R. Yamada, and L. C. L. Yuan, Phys. Rev. Letters **14**, 74 (1965).

[20] L. Kirillova, L. Khristov, V. Nikitin, M. Shafranova, L. Strunov, V. Sviridov, Z. Korbel, L. Rob, P. Markov, Kh. Tchernev, T. Todorov, and A. Zlateva, Phys. Letters **13**, 93 (1964).

[21] J. D. Dowell, R. J. Homer, Q. H. Khan, W. K. McFarlane, J. S. C. McKee, and A. W. O'Dell, *Proceedings of the Sienna International Conference on Elementary Particles and High Energy Physics, 1963*, edited by G. Bernardini and G. P. Puppi (Società Italiana de Fisica, Bologna, 1963), Vol. I, p. 683; Phys. Letters **12**, 252 (1964).

[22] G. Bellettini, G. Cocconi, A. N. Diddens, E. Lillethun, J. Pahl, J. P. Scanlon, J. Walters, A. M. Wetherell, and P. Zanella, Phys. Letters **14**, 164 (1965).

[23] P. Söding, Phys. Letters **8**, 285 (1964).

[24] A. A. Carter and D. V. Bugg, Phys. Letters **20**, 203 (1966).

interference correction (4) into two parts

$$d\sigma(\mathrm{CN})=\int_{\theta_i}^{\theta_5}+\int_{\theta_5}^{\infty}=d\sigma(\mathrm{CN}_1)+d\sigma(\mathrm{CN}_2). \quad (6)$$

θ_i is the angle subtended by the ith counter. In the first term, θ is small enough for the angular dependence of $f(\theta)$ and the form factors for Coulomb scattering to be expanded in a power series in t. Then

$$d\sigma(\mathrm{CN}_1)=(4\pi\alpha\hbar c/p\beta)\,\mathrm{Re}f(0)\ln(t_5/t_i)+At+Bt^2+\cdots.$$

The terms linear and quadratic in t may be taken into the extrapolation to zero solid angle, and only the first term of this correction needs to be made explicitly. Then uncertainty in its magnitude arises only from uncertainty in $\mathrm{Re}f(0)$. Uncertainty in the angular dependence contributes only to the second term, which is smaller. A form factor $\exp(5.5t)$ has been used for the p-p Coulomb amplitude,[25] and $\exp(18.3t)$ for the p-d Coulomb form factor.[26] The second term of (6) then becomes

$$d\sigma(\mathrm{CN}_2)=(-4\pi\alpha\hbar c/p\beta)\,\mathrm{Re}f(0)\,\mathrm{Ei}(\gamma t),$$

where $\gamma=10.1$ and 29 for p-p and p-d scattering, respectively, and $\mathrm{Ei}(-x)$ is the exponential integral function.

The corrections for Coulomb-nuclear interference are large compared with our errors of measurement. They are tabulated in columns 2 and 3 of Tables II and IV. However, at high energies, $\mathrm{Re}f(0)$ is governed largely by the rate of change of the total cross section. In the absence of pronounced structure in the total cross sections, $\mathrm{Re}f(0)$ will change slowly and smoothly with momentum, and is unlikely to affect seriously the shapes of the cross sections deduced from our results.

(vi) Extrapolation to Zero Solid Angle

The partial cross section σ_i recorded by each transmission counter i was determined from the ratio $(t_e/t_f)_i$, and the σ_i were fitted to a power series in the solid angle Ω_i:

$$\sigma_i=A+B\Omega_i+C\Omega_i^2+D\Omega_i^3+\cdots.$$

Since the error on A increases sharply with the number of free parameters in the power series, coefficients C, D, etc., were fixed in various ways. For hydrogen, coefficients D and above were set to zero. For deuterium, Kirillova[27] *et al.* report an angular distribution $\exp(26t)$. The value of D was determined from the power series expansion of this exponential for small t, and a value $d\sigma/d\Omega(0°)$ deduced from the optical theorem; higher powers were negligible. This value of D was small, and the final values obtained for $\sigma(p$-$d)$ are insensitive to its precise value. The aluminum data presented special problems since the extrapolation was very nonlinear. This is discussed in Sec. 5(c).

Preliminary values of A, B, and C were determined by a least-squares fit to the experimental data. Values of C/p^4 when plotted against momentum p, were statistically compatible with a smoothly varying function. A smooth curve was drawn through them, and final values of A and B were determined from a least-squares fit using these smoothed values of C.

(vii) Air Density Variations

Straightforward corrections have been applied for changes in the density of the air between target and counters in the time between target full and empty runs. Only at the highest momentum did they exceed 10 μb.

(viii) Ortho-Para Ratio and Purity of the Deuterium

The hydrogen in the target was completely converted to the *para* state before the run began. However, in deuterium, the conversion to the *ortho* state was slow, even in the presence of a catalyst; it had a time constant of about 100 h, and allowance had to be made for the *ortho-para* ratio in the target liquid. The maximum correction for *para* content in the deuterium was 30 μb. Samples of the deuterium were analyzed in a mass spectrometer and it was found to have an atomic composition of $99.00\pm0.02\%$ deuterium and $1.00\pm0.02\%$ hydrogen. Allowance was made for the hydrogen content in calculating $\sigma(p$-$d)$, assuming that the hydrogen was all in the form of HD.

(ix) Glauber Correction

In deducing $\sigma(p$-$n)$ and $\sigma(I=0)$ from $\sigma(p$-$d)$, allowance has to be made for shadowing of one nucleon by the other in the deuteron. A formula for this effect has been given by Glauber.[28]

$$\sigma(p\text{-}d)=\sigma(p\text{-}p)+\sigma(p\text{-}n)-(1/4\pi)\langle r^{-2}\rangle \times\{\sigma(p\text{-}p)\sigma(p\text{-}n)-(4\pi/k)^2\,\mathrm{Re}f_{pp}(0)\,\mathrm{Re}f_{pn}(0)\}. \quad (7)$$

Experimental values of $\langle r^{-2}\rangle$ have been given by Baker *et al.*[29] as 0.0239 mb^{-1}, and by Galbraith *et al.*[5] as 0.0424 mb^{-1}. The systematic errors in the experimental determinations are comparable with the difference between them. They yield corrections to $\sigma(p$-$d)$ of the order of 3 and 6 mb, respectively. Franco and Glauber[30]

[25] R. Hofstadter, F. Bumiller, and M. Croissiaux, Phys. Rev. Letters **5**, 263 (1960).
[26] J. A. McIntyre and G. R. Burleson, Phys. Rev. **112**, 2077 (1958).
[27] L. F. Kirillova, V. A. Nikitin, V. S. Pantuev, V. A. Sviridov, L. N. Strunov, M. N. Khachaturyan, L. G. Khristov, M. G. Shafranova, Z. Korbel, L. Rob, S. Damyanov, A. Zlateva, Z. Zlatanov, V. Iordanov, Kh. Kanazirski, P. Markov, T. Todorov, Kh. Chernev, N. Dalkhazhav, and T. Tuvdendorzh, Yadern. Fiz. **1**, 533 (1965) [English transl.: Soviet J. Nucl. Phys. **1**, 379 (1965)].
[28] R. J. Glauber, Phys. Rev. **100**, 242 (1955).
[29] W. F. Baker, E. W. Jenkins, T. F. Kycia, R. H. Phillips, A. L. Read, K. F. Riley, and H. Ruderman, *Proceedings of the Sienna Conference on Elementary Particles and High Energy Physics, 1963*, edited by G. Bernardini and G. P. Puppi (Società Italiana di Fisica, Bologna, 1963), Vol. I, p. 634.
[30] V. Franco and R. J. Glauber, Phys. Rev. **142**, 1195 (1966).

TABLE II. Total cross sections for p-p scattering, $\sigma(p\text{-}p)$ and the corrections for Coulomb-nuclear interference. The definitions of $d\sigma(CN_1)$ and $d\sigma(CN_2)$ are given in Eq. (6), Sec. 3(v).

Laboratory momentum (MeV/c)	$d\sigma(CN_1)$ (mb)	$d\sigma(CN_2)$ (mb)	$\sigma(pp)$ (mb)	Total center-of-mass energy (MeV)	Re$f(0)$/Im$f(0)$
1111	0.449	0.280	34.029±0.170	2119	0.55
1289	0.347	0.188	43.234±0.113	2180	0.44
1408	0.206	0.102	46.487±0.052	2222	0.21
1607	−0.026	−0.012	47.476±0.058	2292	−0.03
1660	−0.050	−0.021	47.553±0.058	2311	−0.05
1780	−0.099	−0.047	47.490±0.046	2354	−0.08
1858	−0.119	−0.058	47.455±0.041	2382	−0.12
1940	−0.136	−0.065	47.357±0.046	2410	−0.14
1952	−0.149	−0.068	47.409±0.041	2415	−0.15
2079	−0.166	−0.081	47.224±0.041	2459	−0.18
2212	−0.183	−0.087	46.985±0.046	2505	−0.20
2280	−0.195	−0.094	46.669±0.041	2528	−0.21
2419	−0.219	−0.102	46.130±0.041	2576	−0.24
2450	−0.220	−0.105	45.827±0.041	2586	−0.24
2592	−0.226	−0.107	45.533±0.041	2634	−0.26
2680	−0.232	−0.109	45.331±0.041	2663	−0.27
2704	−0.230	−0.111	45.174±0.041	2671	−0.27
2819	−0.237	−0.112	45.008±0.041	2710	−0.28
2857	−0.255	−0.115	44.928±0.041	2721	−0.28
2958	−0.238	−0.109	44.651±0.041	2755	−0.29
2994	−0.245	−0.117	44.466±0.041	2766	−0.29
3054	−0.248	−0.107	44.401±0.041	2786	−0.30
3110	−0.250	−0.107	44.188±0.041	2804	−0.30
3131	−0.246	−0.119	44.156±0.041	2816	−0.30
3142	−0.246	−0.119	44.114±0.041	2820	−0.30
3277	−0.246	−0.121	43.610±0.041	2857	−0.30
3303	−0.251	−0.120	43.669±0.041	2866	−0.31
3444	−0.251	−0.121	43.138±0.041	2909	−0.31
3546	−0.250	−0.123	42.978±0.037	2941	−0.31
3731	−0.254	−0.122	42.680±0.041	2998	−0.32
3908	−0.272	−0.121	42.316±0.041	3051	−0.33
4037	−0.257	−0.122	42.136±0.041	3090	−0.33
4265	−0.254	−0.122	41.765±0.041	3157	−0.33
4552	−0.255	−0.120	41.457±0.041	3239	−0.34
4783	−0.250	−0.119	41.377±0.037	3303	−0.33
4966	−0.251	−0.121	41.165±0.041	3354	−0.33
5221	−0.253	−0.119	41.171±0.032	3425	−0.33
5526	−0.248	−0.117	40.878±0.041	3505	−0.33
5824	−0.247	−0.117	40.848±0.041	3584	−0.33
7835	−0.228	−0.105	40.075±0.052	4072	−0.32

show, in the impulse approximation, that

$$\langle r^{-2}\rangle=\int_0^{-\infty} dt\, S(t) f_{pp}(\theta) f_{pn}(\theta)/f_{pp}(0) f_{pn}(0).$$

Here $S(t)$ is the form factor of the deuteron. We take $f(\theta)$ to go as $\exp(9.6t)$ for both pp and pn scattering. We have considered two wave functions for the deuteron,[31] (a) a Hulthén wave function

$$\psi(r)=Ne^{-\alpha r}(1-e^{-\lambda r})/r,$$

where $\alpha=0.232$ F^{-1} and $\lambda=1.21$ F^{-1}, and (b) a repulsive-core wave function

$$\psi'(r)=N'e^{-\alpha r}(1-e^{-\gamma r})^3/r$$

with $\gamma=2.21$ F^{-1}. They give values of (a) 0.0340 mb^{-1} and (b) 0.0311 mb^{-1} for $\langle r^{-2}\rangle$. McIntyre and Burleson[26] claim that (b) fits the electron-deuteron scattering data better than (a). Therefore, we have settled on the value

$$\langle r^{-2}\rangle=0.0311 \text{ mb}^{-1}.$$

It is unfortunate that there should be such a large uncertainty in the absolute magnitude of the Glauber correction, and it is clear that a determination of $\sigma(n\text{-}p)$ at one energy to an accuracy better than 1% would be valuable in fixing its magnitude. However, in the first approximation, uncertainty in the value of $\langle r^{-2}\rangle$ affects only the absolute scale of $\sigma(p\text{-}n)$, and does not introduce any spurious structure into it.

[31] L. Durand, III, Phys. Rev. **123**, 1393 (1961).

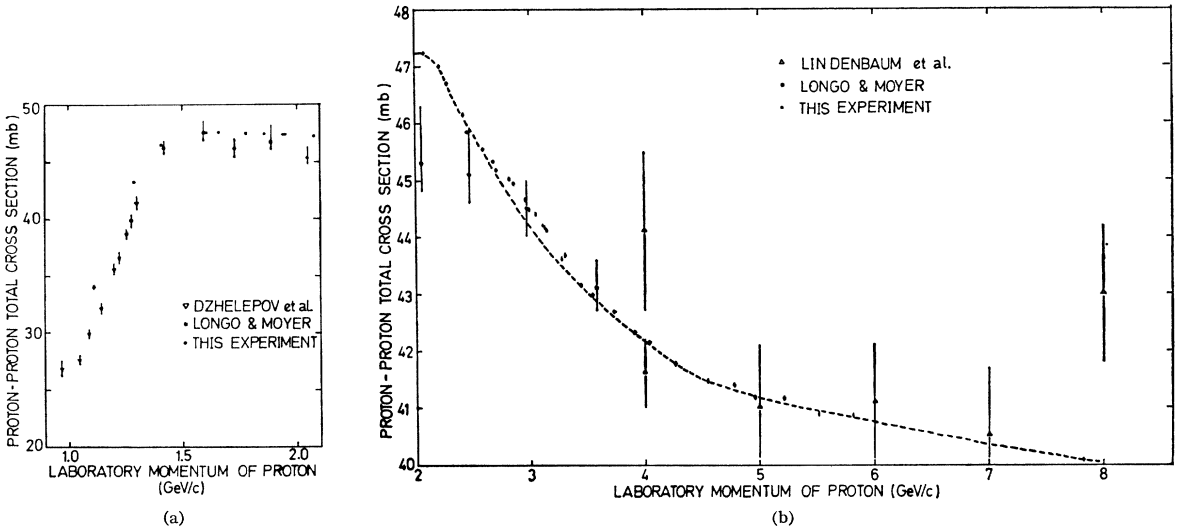

FIG. 5. The total cross section for p-p scattering, $\sigma(p\text{-}p)$ (a) from 1 to 2 GeV/c, (b) up to 8 GeV/c.

(x) Fermi Motion in the Deuteron

Any structure in $\sigma(p\text{-}p)$ or $\sigma(p\text{-}n)$ is smeared out in $\sigma(p\text{-}d)$ by the Fermi motion of the nucleons. This effect can be calculated if the wave function of the deuteron is known. We have calculated it using the two wave functions given in the previous section. Differences between (a) and (b) affect $\sigma(p\text{-}n)$ by less than 50 μb. Values of $\sigma(p\text{-}n)$ and $\sigma(I=0)$ in Table V have therefore been calculated using (b), and column 3 of Table V lists the difference between values of "$\sigma(p\text{-}p)$," the cross section averaged over the Fermi motion, calculated with (a) and (b).

4. THE ASSESSMENT OF ERRORS

Sources of error at any one momentum $\gtrsim \pm 0.01\%$ are listed below, with typical values in brackets:

(i) statistics of the number of particles scattered (0.07%);

(ii) uncertainties in the B and C coefficients used in the extrapolation to zero solid angle (0.06%);

(iii) length of the target (0.03%);

(iv) vapor pressure, and hence density of a target (0.01%);

(v) fluctuations in the density of the air between target and transmission counters due to draughts (0.03%);

(vi) uncertainties in randoms corrections (0.01%).

In addition, there are the following systematic errors, which affect all momenta equally, or which vary only slowly with momentum:

(vii) uncertainty in the relation between vapor pressure and density for liquid hydrogen (0.04%) and deuterium (0.15%);

(viii) uncertainty in the magnitude of the correction for Coulomb-nuclear interference (0.3%);

(ix) uncertainty in the corrections applied in the extrapolation to zero solid angle for cubic and higher terms, due to small angle elastic scattering ($<0.01\%$ for hydrogen and deuterium; 0.5% for aluminum);

(x) uncertainty in the efficiencies with which transmission counters detected scattered particles (0.05%);

(xi) uncertainty in the composition of the deuterium target (0.02%).

In deriving $\sigma(p\text{-}n)$ and $\sigma(I=0)$ there are uncertainties due to:

(xii) uncertainty about $\mathrm{Re}f_{pp}(0)$ and $\mathrm{Re}f_{np}(0)$. This could affect $\sigma(p\text{-}n)$ and $\sigma(I=0)$ over fairly narrow ranges of momentum by 0.5% and 1%, respectively;

(xiii) uncertainty in the absolute magnitude of the Glauber correction produces a systematic error in $\sigma(p\text{-}n)$ and $\sigma(I=0)$ of the order of 2.5% and 5%, respectively;

(xiv) uncertainty in the wave function of the deuteron to be used in correcting for Fermi motion. A guide to this is the difference resulting from the two wave functions we have tried. This difference varies from zero to about 60 μb. Since it changes rapidly with momentum where $\sigma(p\text{-}p)$ and $\sigma(I=0)$ are changing rapidly, it has been added into the errors quoted on $\sigma(p\text{-}n)$ and $\sigma(I=0)$ in columns 4 and 5 of Table V as a systematic error; i.e., it has been added algebraically to the rms statistical error. This probably results in a slight overestimate of these errors.

5. RESULTS

(a) $\sigma(p\text{-}p)$

Values of $\sigma(p\text{-}p)$ are tabulated in column 4 of Table II. The two contributions to the Coulomb-nuclear interference correction are listed in columns 2 and 3.

TABLE III. Individual reaction cross sections in mb observed in bubble-chamber experiments on p-p scattering in the momentum range 1.6 to 3.7 GeV/c. (π mesons are denoted by their charges in the first column.)

Final state \ Momentum (GeV/c)	1.66	2.23	2.81	3.68
pp	24.9 ±0.6	20.27±0.7	17.97 ±0.45	15.60 ±0.77
inelastic	22.6 ±0.6	26.58±0.7	27.03 ±0.45	27.11 ±0.77
$pn+$	18.4 ±0.7	17.57±0.6	15.02 ±0.41	11.65 ±0.66
$pp0$	3.7 ±0.3	4.06±0.27	3.60 ±0.21	2.95 ±0.31
$d+$	0.48±0.08	0.13±0.05	0.16 ±0.04	0.11 ±0.06
$d+0$	0.01±0.01	0.44±0.08		···
$nn++$	0	0.26±0.06	0.58 ±0.08	···
$pp00$	0	0.42±0.08	0.86 ±0.10	···
$pn+0$	0	2.42±0.20	3.81 ±0.20	···
$pp+-$	0.01±0.01	1.24±0.14	2.35 ±0.14	2.72 ±0.13
$pp+-0$	0	0.02±0.02	0.20 ±0.03	0.75 ±0.07
$pn++-$	0	···	0.38 ±0.04	1.17 ±0.09
$d++-$	0	···	0.05 ±0.05	0.07 ±0.02
multiple pion	<0.1	4.80	8.23 ±0.3	7.50 ±0.52
strange particles	0	···	0.018±0.005	0.178±0.032
$NN^*(1238)$	22.1	~18.9	16.3 ±1.2	⩾7.3
$N(N^*(1512)$ or $N^*(1688))$	0	~2.7	3.3 ±1.8	small
$N^*(1238)(N^*(1512)$ or $N^*(1688))$	0	0	~1.7	···
ppn	0	···	0.55	···
$pn+/pp0$	4.97	4.33	4.17	3.95

The results are plotted in Fig. 5, together with results from three previous experiments spanning the region. In general, the agreement with other experiments is within the errors. However, our lowest two momentum points appear to be significantly higher than previous ones. Part of the discrepancy arises from our results being corrected (upwards) for Coulomb-nuclear interference. After allowing for this however, some discrepancy remains, and is probably due to a small disagreement in momentum scale.

Some structure is evident in $\sigma(p$-$p)$ between momenta of 2.5 and 3.3 GeV/c. The dashed curve, which is an estimate made by eye of what a smooth background might be, leaves a cross section of about 0.4 mb in a peak centered at about 3 GeV/c. However, the background estimate is highly subjective, and the remaining structure could differ in magnitude by a factor of two either way.

We have suggested in an earlier letter[32] that this structure could be due either to the rapid onset of an inelastic process, such as $N^*(1688)$ production, or to the existence of a di-baryon resonance at a mass of 2.75 GeV/c^2. We wish to pursue these two possibilities a little further here.

Mandelstam[33] and Ferrari and Selleri[34] have shown that the rapid rise in $\sigma(p$-$p)$ between 1 and 1.5 GeV/c may be explained by $N^*(1238)$ production via single-pion exchange. It is remarkable that $N^*(1512)$ and $N^*(1688)$ production do not similarly produce large effects in the total cross section. However, because the Clebsch-Gordan coefficients are small in the matrix element for production of an $I=\frac{1}{2}$ isobar, single-pion exchange is responsible for cross sections of only about 1.5 and 1.2 mb for $N^*(1512)$ and $N^*(1688)$ production just above threshold. The latter figure is rather bigger than the peak we observe at 3 GeV/c. In Table III, we collect individual reaction cross sections observed in bubble chamber experiments spanning this range[35–38]; they have all been normalized to the total cross sections reported here. It is clear that $N^*(1238)$ production dominates p-p inelastic scattering in this region, and production of higher isobars is strongly suppressed. The peak in $\sigma(p$-$p)$ at 3 GeV/c is so small that it cannot be identified with any particular reaction in Table III; it would certainly be compatible with $N^*(1688)$ production. If so, one might look for evidence of $N^*(1512)$ production at or near its threshold energy. There is some sign of a shoulder in $\sigma(p$-$p)$ at about 2 GeV/c,

[32] R. F. George, K. F. Riley, R. J. Tapper, D. V. Bugg, D. C. Salter, and G. H. Stafford, Phys. Rev. Letters **15**, 214 (1965).
[33] S. Mandelstam, Proc. Roy. Soc. (London) **A244**, 491 (1958).
[34] E. Ferrari and F. Selleri, Nuovo Cimento **27**, 1450 (1963).
[35] G. A. Smith, H. Courant, E. C. Fowler, H. Kraybill, J. Sandweiss, and H. Taft, Phys. Rev. **123**, 2160 (1961).
[36] W. J. Fickinger, E. Pickup, D. K. Robinson, and E. O. Salant, Phys. Rev. **125**, 2082 and 2091 (1962).
[37] D. V. Bugg, A. J. Oxley, J. A. Zoll, J. G. Rushbrooke, V. E. Barnes, J. B. Kinson, W. P. Dodd, G. A. Doran, and L. Riddiford, Phys. Rev. **133**, B1017 (1964).
[38] A. M. Eisner, E. L. Hart, R. I. Louttit and T. W. Morris, Phys. Rev. **138**, B670 (1965).

although its interpretation depends heavily on what cross section is attributed to $N^*(1238)$ production. According to Table III, the cross-section for double-pion production rises rapidly in this region, offsetting the decrease in the elastic cross section and keeping the total cross section roughly constant. Either double $N^*(1238)$ production or $N^*(1512)$ production with subsequent decay into $N\pi\pi$ could account for this.[39]

A second possibility is that the peak at 2.75 GeV/c^2 is due to a di-baryon resonance. Then the smallest $SU(3)$ representation into which it could be fitted is the **27**. This representation would also contain two $Y=1$ states with $I=\frac{1}{2}$ and $\frac{3}{2}$, which should presumably appear as ΛN or ΣN resonances. There have been reports of $Y=1$ resonances at 2.098 GeV/c^2 [40] and at 2.36 GeV/c^2 [41]; these were not observed in a recent experiment by Melissinos *et al.*,[42] but there was instead a peak at 2.05 GeV/c^2 very close to the ΛN threshold. All these mass values are well below the position of the 2.75 GeV/c^2 peak observed here.

(b) $\sigma(p\text{-}n)$ and $\sigma(I=0)$

Values of $\sigma(p\text{-}d)$ after correction for Coulomb-nuclear interference are tabulated in column 4 of Table IV. In deducing $\sigma(p\text{-}n)$ and $\sigma(I=0)$, the following steps are involved. First "$\sigma(p\text{-}p)$" is calculated, namely the value of $\sigma(p\text{-}p)$ averaged over the Fermi motion of the target proton in the deuteron. Then $\sigma(p\text{-}d)-$"$\sigma(p\text{-}p)$" is derived, and from that "$\sigma(p\text{-}n)$" using the Glauber correction. Next "$\sigma(I=0)$" is obtained as 2"$\sigma(p\text{-}n)$" $-$"$\sigma(p\text{-}p)$". $\sigma(I=0)$ is obtained by fitting a curve by eye to "$\sigma(I=0)$" and unfolding from it the Fermi motion. Then

$$\sigma(p\text{-}n)=\tfrac{1}{2}\sigma(I=0)+\tfrac{1}{2}\sigma(p\text{-}p).$$

This value should, of course, agree with a value obtained from "$\sigma(p\text{-}n)$" by unfolding the Fermi motion. However, such is the bias of the eye in fitting smooth curves that we have found values determined in these two ways to differ quite significantly. Since $\sigma(p\text{-}n)$ contains any structure resulting from both $I=1$ and $I=0$ states, we prefer the derivation outlined above.

Values of "$\sigma(p\text{-}n)$" and "$\sigma(I=0)$" are given in Table V, and plotted in Figs. 6 and 7. The dashed curve is obtained by fitting "$\sigma(I=0)$" by eye, and the full curves result from it by unfolding the Fermi motion. The values of $\sigma(p\text{-}n)$ and $\sigma(I=0)$ obtained by this unfolding process depend strongly on the dashed curves which are fitted to the experimental results. This is illustrated in Fig. 8, where two small inflections in the experimental values of "$\sigma(I=0)$" at 2.2 and 3.5 GeV/c are followed by the solid curve; this then generates the pronounced bumps in the dashed curve, when the Fermi motion is unfolded. It is clear that structure of this order of magnitude in $\sigma(I=0)$ could well escape detection in total cross section experiments where deuterium is used as a target. To determine $\sigma(p\text{-}n)$ and $\sigma(I=0)$ better than has been done here, it seems necessary to eliminate the Fermi motion. This might be achieved by accelerating deuterons, scattering them in a hydrogen target, and recording the momentum spectrum of "spectator" protons stripped from the deuteron when the neutron interacts. There would, of course, be the further complication that sometimes the deuteron would not break up, particularly in small-angle elastic scattering. It would be possible, and indeed desirable, to infer $\mathrm{Re}f_{np}(0)$ from Coulomb-nuclear interference in the elastic d-p scattering.

Our experimental results do not establish structure in $\sigma(I=0)$ other than the long rise from 1.6 to 3 GeV/c

TABLE IV. Total cross sections for p-d scattering, $\sigma(p\text{-}d)$. Columns are as for Table II.

Laboratory momentum (MeV/c)	$d\sigma(\mathrm{CN}_1)$ (mb)	$d\sigma(\mathrm{CN}_2)$ (mb)	$\sigma(p\text{-}d)$ (mb)	$[\mathrm{Re}f(0)/\mathrm{Im}f(0)]_{pn}$
1111	0.326	0.230	67.209±0.090	−0.11
1289	0.162	0.135	76.905±0.110	−0.25
1408	−0.034	0.048	80.490±0.057	−0.31
1607	−0.309	−0.066	82.472±0.063	−0.38
1660	−0.324	−0.059	82.889±0.063	−0.39
1780	−0.492	−0.119	83.377±0.052	−0.41
1858	−0.423	−0.116	84.039±0.047	−0.42
1940	−0.456	−0.121	84.260±0.046	−0.44
1952	−0.468	−0.139	84.280±0.047	−0.44
2079	−0.485	−0.137	84.526±0.047	−0.46
2212	−0.508	−0.142	84.524±0.047	−0.47
2280	−0.533	−0.154	84.624±0.047	−0.47
2450	−0.569	−0.165	84.239±0.047	−0.48
2592	−0.572	−0.158	84.212±0.047	−0.49
2680	−0.575	−0.164	84.085±0.044	−0.50
2704	−0.572	−0.169	83.912±0.047	−0.50
2819	−0.580	−0.165	83.846±0.047	−0.50
2857	−0.609	−0.166	83.790±0.047	−0.50
2958	−0.577	−0.160	83.602±0.047	−0.51
2994	−0.593	−0.168	83.452±0.047	−0.51
3054	−0.596	−0.153	83.289±0.047	−0.51
3110	−0.600	−0.154	83.328±0.047	−0.51
3142	−0.595	−0.178	83.166±0.047	−0.51
3277	−0.592	−0.180	82.489±0.047	−0.51
3303	−0.599	−0.170	82.730±0.047	−0.51
3444	−0.597	−0.178	81.960±0.047	−0.51
3546	−0.593	−0.182	81.710±0.047	−0.51
3908	−0.632	−0.174	81.107±0.033	−0.51
4037	−0.591	−0.176	80.930±0.047	−0.51
4265	−0.585	−0.170	80.417±0.047	−0.50
4552	−0.579	−0.169	80.125±0.047	−0.50
4966	−0.566	−0.172	79.632±0.047	−0.49
5221	−0.566	−0.166	79.578±0.037	−0.48
5526	−0.558	−0.168	79.316±0.047	−0.48
5824	−0.548	−0.165	79.091±0.047	−0.47
7835	−0.496	−0.145	77.858±0.052	−0.43

[39] E. Ferrari, Nuovo Cimento **30**, 240 (1963).
[40] H. O. Cohn, K. H. Bhatt and W. M. Bugg, Phys. Rev. Letters **13**, 668 (1964).
[41] P. A. Piroué, Phys. Letters **11**, 164 (1964).
[42] A. C. Melissinos, N. W. Reay, J. T. Reed, T. Yamanouchi, E. Sacharidis, S. J. Lindenbaum, S. Ozaki, and L. C. L. Yuan, Phys. Rev. Letters **14**, 604 (1965).

TABLE V. Total cross section for p-n scattering, and in the $I=0$ state. Columns headed "σ" are cross sections averaged over the Fermi motion of the target particle; those headed σ have the Fermi motion unfolded. Column 3 lists the systematic error in "$\sigma(p$-$p)$ arising from uncertainty in the deuteron wave function, as described in Sec. 4 (xiv) of the text. The errors quoted in subsequent columns are random errors plus a systematic error propagated from column 3.

Laboratory momentum (MeV/c)	"$\sigma(p$-$p)$" (mb)	Δ"$\sigma(p$-$p)$" (systematic) (mb)	"$\sigma(p$-$n)$" (mb)	"$\sigma(I=0)$" (mb)	$\sigma(I=0)$ (mb)	$\sigma(p$-$n)$ (mb)	Total center-of-mass energy (MeV)
1111	34.684	0.058	35.72 ±0.26	36.75±0.75	36.41	35.22	2119
1289	42.851	0.030	38.64 ±0.20	34.42±0.52	34.29	38.76	2180
1408	45.886	0.052	39.44 ±0.14	32.99±0.38	32.74	39.61	2222
1607	47.327	0.039	39.77 ±0.13	32.22±0.36	31.75	39.61	2292
1660	47.422	0.033	40.09 ±0.13	32.76±0.35	32.38	39.97	2311
1780	47.438	0.024	40.559±0.104	33.68±0.26	33.53	40.51	2354
1858	47.410	0.021	41.224±0.090	35.04±0.23	34.95	41.20	2382
1940	47.298	0.019	41.530±0.090	35.76±0.24	35.72	41.54	2410
1952	47.347	0.018	41.479±0.087	35.61±0.22	35.57	41.49	2415
2079	47.129	0.016	41.905±0.085	36.68±0.22	36.67	41.95	2459
2212	46.809	0.024	42.174±0.092	37.54±0.26	37.56	42.27	2505
2280	46.560	0.013	42.500±0.081	38.44±0.21	38.47	42.57	2528
2450	45.847	0.009	42.684±0.077	39.52±0.20	39.56	42.69	2586
2592	45.539	0.008	42.890±0.076	40.24±0.19	40.28	42.91	2634
2680	45.305	0.008	42.961±0.074	40.62±0.19	40.66	43.00	2663
2704	45.143	0.008	42.933±0.076	40.72±0.19	40.76	42.97	2671
2819	44.958	0.008	43.017±0.076	41.08±0.19	41.12	43.06	2710
2857	44.863	0.008	43.037±0.076	41.21±0.19	41.25	43.09	2721
2958	44.565	0.008	43.113±0.076	41.66±0.19	41.69	43.17	2755
2994	44.383	0.008	43.115±0.076	41.85±0.19	41.88	43.17	2766
3054	44.322	0.008	42.979±0.076	41.64±0.19	41.67	43.04	2786
3110	44.118	0.007	43.226±0.075	42.33±0.19	42.36	43.27	2804
3142	44.047	0.006	43.118±0.074	42.19±0.18	42.22	43.17	2820
3277	43.570	0.004	42.812±0.072	42.03±0.18	42.06	42.84	2857
3303	43.667	0.004	42.986±0.072	42.31±0.18	42.33	43.00	2866
3444	43.205	0.002	42.582±0.070	41.96±0.18	41.98	42.56	2909
3546	42.996	0.001	42.522±0.069	42.05±0.16	42.07	42.52	2941
3908	42.300	0	42.525±0.057	42.75±0.15	42.77	42.56	3051
4037	42.128	0	42.495±0.068	42.86±0.17	42.88	42.51	3090
4265	41.790	0.001	42.276±0.069	42.76±0.17	42.78	42.27	3157
4552	41.486	0.001	42.255±0.069	43.03±0.17	43.03	42.24	3239
4966	41.161	0	42.069±0.068	42.98±0.17	42.99	42.08	3354
5221	41.161	0.001	42.017±0.053	42.87±0.13	42.88	42.03	3425
5526	40.872	0.001	42.034±0.069	43.19±0.17	43.20	42.04	3505
5824	40.842	0.001	41.821±0.070	42.80±0.17	42.81	41.83	3584
7835	40.074	0	41.328±0.080	42.58±0.20	42.59	41.33	4072

which is presumably due to the onset of strong inelastic processes. It is interesting that $\sigma(I=0)$ and $\sigma(p$-$p)$ both appear to flatten out between about 4 and 5 GeV/c.

Our values of $\sigma(p$-$d)$ are compared with those of earlier experiments on Fig. 9. Our results appear to be $\sim$2 mb systematically higher than those of Galbraith *et al.* Even if our deuterium were 100% pure, this would reduce our cross sections only by 0.5 mb below those shown on the figure. This disagreement in $\sigma(p$-$d)$ is surprising in view of the good agreement on $\sigma(p$-$p)$, but some of it may perhaps be traced to the different ranges of transverse momentum intercepted by the transmission counters in the two experiments. In Ref. 5 the smallest counter accepted particles with transverse momenta up to 140 MeV/c, compared to 70 MeV/c in the present experiment. Since the elastic p-d scattering falls approximately as $\exp(26t)$ at these energies, it may be that a significant fraction of the elastically scattered beam was detected by the transmission counters in Ref. 5 resulting in a lower extrapolated cross section. Calculation shows, however, that this does not explain all of the discrepancy.

(c) Aluminum Cross Sections

The aluminum nucleus is expected to have a radius of about 4 F. If it scatters as a grey disk, the first diffraction minimum will occur at a transverse momentum of about $p_T=180$ MeV/c. In this experiment, the transmission counters covered a range of about $p_T=50$ to 140 MeV/c; i.e., they straddled the angular region where elastic (or quasielastic) scattering was important. The consequences of this were that (i) the extrapolation to zero solid angle was very nonlinear, (ii) it was possible to get some idea of the elastic cross section from the form of the extrapolation.

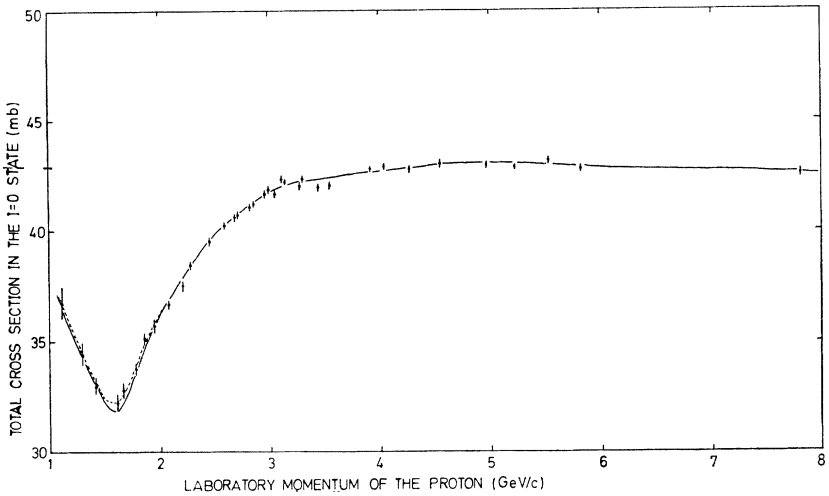

FIG. 6. The total cross section for scattering in the $I=0$ state. The dotted curve is a fit made by eye to the experimental points; the solid curve is obtained from it by unfolding the Fermi motion.

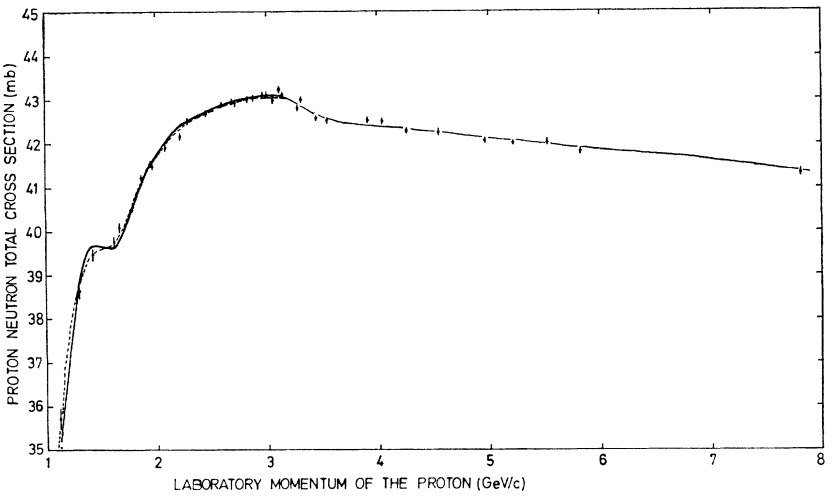

FIG. 7. The total cross section for p-n scattering. The full curve shows the result of unfolding the Fermi motion as described in the text.

In the small angular range covered by the transmission counters, debris from disintegration of the aluminum nucleus should be approximately isotropic. We have therefore tried to fit the data with two forms:

$$\frac{d\sigma}{d\Omega}=\alpha\left\{\frac{J_1(kR\sin\theta)}{kR\sin\theta}\right\}^2+\beta, \tag{8a}$$

and

$$\frac{d\sigma}{d\Omega}=\alpha' \exp\{\tfrac{1}{8}k^2R^2\sin^2\theta\}+\beta'. \tag{8b}$$

The value of R turned out to be quite well determined and independent of momentum, namely $R=4.1\pm0.1$ F. However, neither form fitted the experimental data within several standard errors. We estimate that there could be systematic errors in our determinations of the total and elastic cross sections of ±5 and ±10 mb, re-

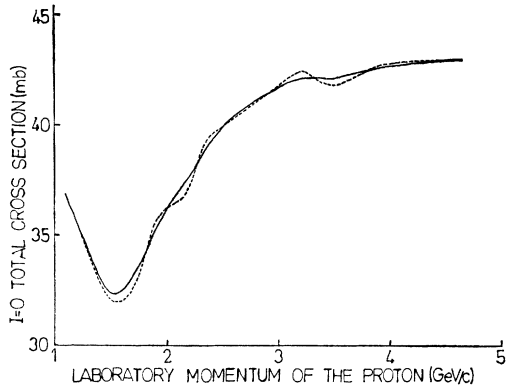

FIG. 8. This figure illustrates the sensitivity of $\sigma(I=0)$ to small bumps in the experimental data when the Fermi motion is unfolded. The solid curve is fitted to the experimental data and includes two small bumps at 2.2 and 3.5 GeV/c. The dashed curve results from unfolding the Fermi motion.

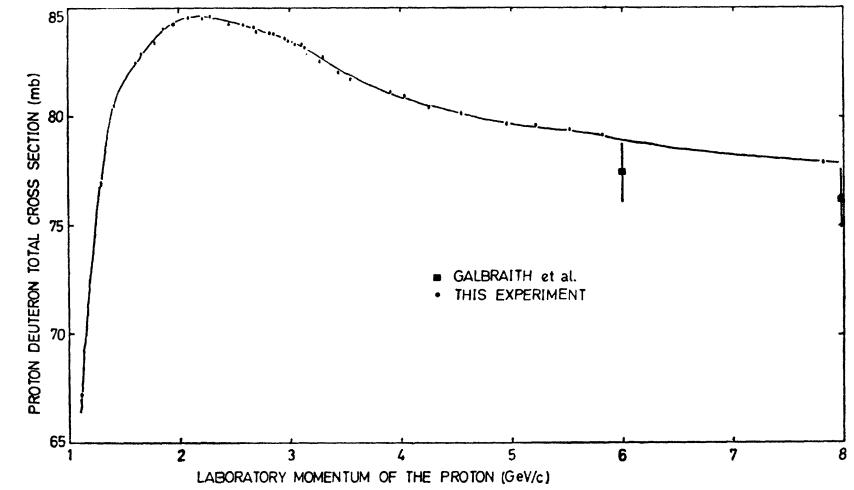

FIG. 9. The total cross section for p-d scattering, $\sigma(p\text{-}d)$.

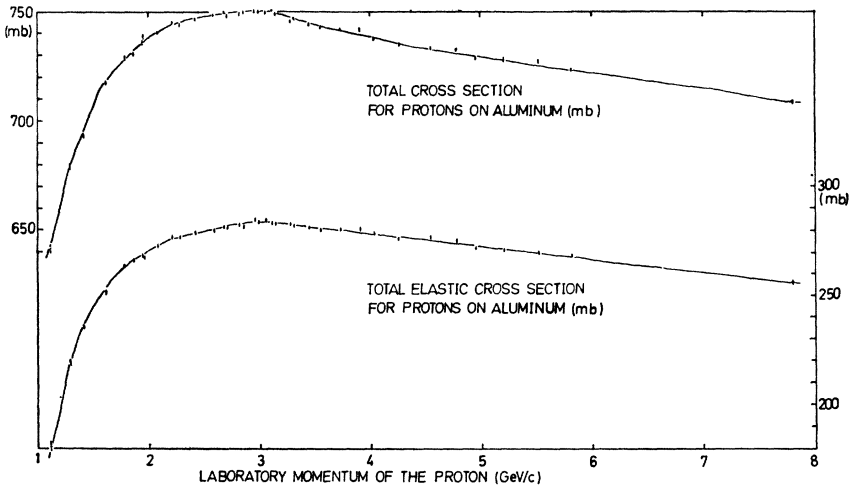

FIG. 10. The total (left-hand scale) and elastic (right-hand scale) cross sections for the scattering of protons by aluminum. The errors shown are purely statistical.

spectively. Furthermore, the systematic errors might change gradually with momentum. With these reservations, we display our values for the total and elastic cross sections in Fig. 10. Both follow the trend of the nucleon-nucleon total cross sections, but show a much smaller variation with momentum. It is rather surprising that most of the variation of the cross section seems to occur in the quasielastic cross section.

ACKNOWLEDGMENTS

We wish to acknowledge the generous assistance and cooperation of the operating staff at Nimrod and the High Energy Physics Engineering Group of the Rutherford Laboratory, in carrying out this experiment. We would like to thank J. Hawkyard, R. Stokoe and P. Hey for their work on the design, construction and operation of the hydrogen and deuterium targets. The technical help given by G. T. J. Arnison and R. Mackenzie is gratefully acknowledged. Miss K. M. Knight gave invaluable assistance in the early stages of preparing this experiment. We are grateful to J. Cresswell, M. Evans and S. Maskell for the enthusiasm with which they assisted us with the electronics. We are indebted to A. E. Taylor and his group for their work in setting up the beam line.

Two of us (R. F. G. and R. J. T.) wish to thank the D. S. I. R./S. R. C. for financial support.